AIAA JOURNAL
Vol. 34, No. 10, October 1996

Partitioned Model Reduction for Large Space Structural Control Problem

Xiaojian Liu* and Junjiro Onoda†
Institute of Space and Astronautical Science, Kanagawa 229, Japan

A model reduction method for control system design of large space structures is presented. The control model of the structure is partitioned into several subdomains, and a generalized Craig–Bampton representation is derived. In considering the placement of actuators/sensors that may affect the selection of the candidate modes, the representative degrees of freedom (DOF) of the actuators/sensors are retained as physical DOF in the final coordinate vector. A reduced model for the controller design is obtained based on this representation. As an example, a space truss subject to four actuator forces is analyzed. Comparison with a conventional reduction method based on a complete model of the truss has been made via eigenpairs and dynamic responses. Good agreement is seen to be achieved, and improved accuracy is obtained with the proposed method. The importance of the actuator/sensor related DOF and the effectiveness of the proposed approach in dealing with the very localized DOF are investigated under the extreme condition where only these four actuator/sensor related DOF are considered as the dimension for the model reduction.

Introduction

IN space engineering an increasingly important consideration in the design of control systems for large space structures (LSS) is economical model preprocessing. This research area has become very attractive, of late, and now sees a large proportion of literature devoted to partition techniques and modal space reduction methods for optimal control purposes. Partitioned approaches have found favor in the simultaneous analysis of control-structure interaction,[1,2] in which several computational aspects and discipline-oriented models are involved. In this circumstance, it may be impossible to put all of the analysis aspects into a single set of governing equations. Modal space reduction is quite intuitive; one problem, however, is that direct superposition of lower-order modes may lose the local structural dynamic behavior, which could seriously affect the design of the control system. In fact, the selection of suitable modes must be subject to such criteria that the reduced model can fully represent the system as accurately as the original. There are two typical modal selection methods based on internal balancing theory[3] and modal cost analysis.[4] However, an essential implication of these methods is that all of the eigenpairs of an LSS are obtained in advance so that selection can be made. For most practical LSS, this is obviously an intractable task.

The well-developed component mode synthesis (CMS) technique has been used in the mechanical and aerospace industry for structural analysis involving eigenvalue problems since the 1960s. For some time, the Craig–Bampton (CB) representation[5] has been widely used with this technique. In more recently developed methods for control system design of space structures,[6,7] the CMS method has been shown to be effective. This paper presents a partitioned approach to the CMS technique for model reduction of control system design for LSS. The study has been motivated by research on active/semiactive vibration suppression[8] with simultaneous optimization and control.[9] First, the model of an LSS may be repeated or periodical, which can be solved economically, or may be a coupled-field problem (e.g., a system with local nonlinearities, or a flexible multibody system with constraints, or a system coupled with electric and thermal fields), where it is preferable to weaken the coupling by domain partition, and then use an existing single-field solver on these individual domains. Second, the traditional CB-based CMS deals with substructures, enforcing compatible interfaces of each of them. Consequently, on assembly of these substructures, all of the information concerning the substructures must be processed. Most importantly, the traditional CMS cannot consider placement of actuator and sensor and the concomitant benefits in control system design. The technique being presented herein separates the LSS into subdomains and then for each subdomain a CB representation is employed with displacement of adjacent subdomains being considered to be boundary displacements. Since the actuator and sensor placement may dominate the selection of the candidate modes, the actuator and sensor associated degrees of freedom (DOF) are taken into account by retaining them as physical DOF in the final generalized coordinate vector. This results in a modified CB representation from which a full rank transformation is derived for the model reduction of the controlled LSS. To demonstrate the effectiveness of this reduced model, a space truss with four actuator forces is solved. Comparison with a conventional model reduction method is made via evaluated eigenpairs and observed truss response.

Partition of Structural Control Model

The general second-order form of a linear and time-invariant structural control model may be written as

$$\begin{aligned} M\ddot{D} + C\dot{D} + KD &= B_0 u \\ Y &= S_1 D + S_2 \dot{D} \end{aligned} \tag{1}$$

where $\boldsymbol{M}$, $\boldsymbol{C}$, and $\boldsymbol{K}$ are the mass, damping, and stiffness matrices. The vector $\boldsymbol{Y}$ is the measurement of observed displacements and velocities from the sensors; and S_1 and S_2 are, respectively, the matrices locating displacement and velocity sensors at nodal DOF. The system is regulated by a vector of control input $\boldsymbol{u}$ via matrix $\boldsymbol{B}_0$.

Suppose the structure is divided into N_s subdomains. The following partitioning of $\boldsymbol{D}$ and the matrices of Eq. (1) are

$$D = \begin{Bmatrix} d_1 \\ d_2 \\ \vdots \\ d_{N_s} \end{Bmatrix}, \qquad M = \begin{bmatrix} m_1 & m_{12} & \cdots & m_{1N_s} \\ m_{21} & m_2 & & m_{2N_s} \\ \vdots & & \ddots & \vdots \\ m_{N_s1} & m_{N_s2} & \cdots & m_{N_s} \end{bmatrix}$$

$$C = \begin{bmatrix} c_1 & c_{12} & \cdots & c_{1N_s} \\ c_{21} & c_2 & & c_{2N_s} \\ \vdots & & \ddots & \vdots \\ c_{N_s1} & c_{N_s2} & \cdots & c_{N_s} \end{bmatrix}$$

Received Nov. 27, 1995; revision received June 6, 1996; accepted for publication June 7, 1996.

*Foreign Research Fellow, Research Division of Space Transportation, 3-1-1 Yoshinodai, Sagamihara; on leave from Dalian University of Technology, People's Republic of China; currently Senior Researcher, Department of Civil Engineering, University of Portsmouth, Burnaby Building, Burnaby Road, Portsmouth PO1 3QL, England, United Kingdom.

†Professor, Research Division of Space Transportation. Member AIAA.

$$K = \begin{bmatrix} k_1 & k_{12} & \cdots & k_{1N_s} \\ k_{21} & k_2 & & k_{2N_s} \\ \vdots & & \ddots & \vdots \\ k_{N_s1} & k_{N_s2} & \cdots & k_{N_s} \end{bmatrix}, \qquad B_0 = \begin{bmatrix} b_{01} \\ b_{02} \\ \vdots \\ b_{0N_s} \end{bmatrix}$$

The equation of motion of the ith subdomain can be written as

$$m_i\ddot{d}_i + c_i\dot{d}_i + k_i d_i + \sum_{j\neq i}^{N_s} c_{ij}\dot{d}_j + \sum_{j\neq i}^{N_s} k_{ij} d_j = b_{0i} u \tag{2}$$

A lumped-mass matrix is assumed such that $m_{ij} = (m_{ji})^T = 0$ for $i \neq j$. Note that the influence on the ith subdomain is limited to the boundary displacements of its related subdomains, indicating that the matrices k_{ij} and c_{ij} should be zero if $j \notin J_i$, where J_i is an adjacent set of the ith subdomain.

Equation (2) is an explicit equation of motion for the ith subdomain, which can be seen to be more straightforward than the traditional CMS.

CB Representation with Consideration of Actuators/Sensors Location

The vector d_i is partitioned into a subset of ordinary displacements d_i^o and a subset of actuator/sensor displacements expressed by $d_i^s \in R^{n_{is}}$. The latter may be important in control system design and should be retained as physical DOF in the final generalized coordinate vector. Compared with d_i^o, d_i^s is usually characteristic of some localized displacements with smaller dimension n_{is}. The partitioning of d_i yields (damping being neglected)

$$\begin{bmatrix} m_i^o & m_i^{os} \\ m_i^{so} & m_i^s \end{bmatrix} \begin{Bmatrix} \ddot{d}_i^o \\ \ddot{d}_i^s \end{Bmatrix} + \begin{bmatrix} k_i^o & k_i^{os} \\ k_i^{so} & k_i^s \end{bmatrix} \begin{Bmatrix} d_i^o \\ d_i^s \end{Bmatrix} + \sum_{j\neq i}^{N_s} \begin{bmatrix} k_{ij}^o \\ k_{ij}^s \end{bmatrix} \{d_j\} = 0 \tag{3}$$

where $m_i^{os} = (m_i^{so})^T = 0$ for a lumped-mass matrix.

Consider the upper partition of the static portion of Eq. (3). The contribution of the constrained modes, denoted as d_i^{ocm}, may be represented by

$$d_i^{ocm} = \varphi_i^s d_i^s + \sum_{j\neq i}^{N_s} \tilde{\varphi}_{ij} d_j \tag{4}$$

where $\varphi_i^s = -(k_i^0)^{-1} k_i^{0s}$ and $\tilde{\varphi}_{ij} = -(k_i^0)^{-1} k_{ij}^0$ are the constrained mode matrices.

The constrained normal modes of the ith subdomain can be obtained from the eigenvalue problem of Eq. (3) with d_i^s and all of the d_j being totally constrained, i.e.,

$$k_i^o \bar{\phi}_i^o - \lambda^o m_i^o \bar{\phi}_i^o = 0 \tag{5}$$

where $(\lambda^o, \bar{\phi}_i^o)$ is an eigenpair of Eq. (5) and $\bar{\phi}_i^{o^T} m_i^o \bar{\phi}_i^o = 1$. It is assumed that d_i^o contains a reasonably large number of displacements and can be approximated by

$$d_i^{onm} = \phi_i^o q_i \tag{6}$$

where $q_i \in R^{n_{iq}}$ is a small set of modal coordinates and accordingly ϕ_i^o is a truncated eigenmode matrix. According to Craig and Bampton,[5] the displacement d_i^o may be expressed as

$$d_i^o = d_i^{ocm} + d_i^{onm} = \phi_i^o q_i + \varphi_i^s d_i^s + \sum_{j\neq i}^{N_s} \tilde{\varphi}_{ij} d_j \tag{7}$$

Let

$$\eta_i = \begin{Bmatrix} q_i \\ d_i^s \end{Bmatrix}$$

be the final coordinate vector of the subdomain and

$$T_i = \begin{bmatrix} \phi_i^o & \varphi_i^s \\ 0 & I \end{bmatrix}$$

the transformation matrix between d_i and η_i is then

$$d_i = \begin{Bmatrix} d_i^o \\ d_i^s \end{Bmatrix} = T_i \eta_i + \begin{bmatrix} \tilde{\varphi}_{i1} & \tilde{\varphi}_{i2} & \cdots & \tilde{\varphi}_{iN_s} \\ 0 & 0 & \cdots & 0 \end{bmatrix} \begin{Bmatrix} d_1 \\ d_2 \\ \vdots \\ d_{N_s} \end{Bmatrix} \tag{8}$$

Equation (8) is a general expression for d_i in terms of η_i and the displacements of all subdomains. Note that the entries $\tilde{\varphi}_{ij}$ $(j = 1, 2, \ldots, N_s)$ should be zero if $j \notin J_i$. Furthermore, because only the boundary displacements of the adjacent subdomains have contribution to d_i, the coefficient matrix of the second term of Eq. (8) may be a highly sparse matrix.

Because of actuator/sensor involvement, the CB representation, Eq. (8), is expected to give more flexibility in control system design. It should be pointed out that the possible displacement vectors d_i^s $(i = 1, 2, \ldots, N_s)$ may be not only the actuator/sensor related nodal DOF but also some other significant DOF that, in the opinion of the designer, is important to the control system design.

Mode Synthesis

Rearranging Eq. (8) for all of the N_s subdomains gives

$$(I - \tilde{\Psi})D = \tilde{T}\eta \tag{9}$$

where

$$\eta = \begin{Bmatrix} \eta_1 \\ \eta_2 \\ \vdots \\ \eta_{N_s} \end{Bmatrix}, \qquad \tilde{T} = \begin{bmatrix} T_1 & & & \\ & T_2 & & \\ & & \ddots & \\ & & & T_{N_s} \end{bmatrix}$$

$$\tilde{\Psi} = \begin{bmatrix} 0 & \tilde{\varphi}_{12} & \tilde{\varphi}_{13} & \cdots & \tilde{\varphi}_{1N_s} \\ 0 & 0 & 0 & & 0 \\ \tilde{\varphi}_{21} & 0 & \tilde{\varphi}_{23} & & \tilde{\varphi}_{2N_s} \\ 0 & 0 & 0 & & 0 \\ \vdots & & & & \\ \tilde{\varphi}_{N_s1} & \tilde{\varphi}_{N_s2} & \tilde{\varphi}_{N_s3} & & 0 \\ 0 & 0 & 0 & \cdots & 0 \end{bmatrix}$$

It is not difficult to prove that $I - \tilde{\Psi}$ has an inverse, but, in general, it is nonsymmetric. This means that it is difficult to evaluate $(I - \tilde{\Psi})^{-1}$ directly. However, if the prescribed actuator/sensor displacements of the subdomains are not on the boundaries of the subdomains, i.e., $d_i^s \cap d_i^b = \emptyset$ $(i = 1, 2, \ldots, N_s)$, where d_i^b is the vector of boundary displacements of the ith subdomain, the calculation of $(I - \tilde{\Psi})^{-1}$ can be significantly simplified.

Theorem: The inverse of $I - \tilde{\Psi}$ in Eq. (9) is $(I - \tilde{\Psi})^{-1} = K_m^{-1} K_d$ if $d_i^s \cap d_i^b = \emptyset$ $(i = 1, 2, \ldots, N_s)$, where

$$K_d = \begin{bmatrix} k_1^o & & & & & & & \\ & k_1^s & & & & & & \\ & & k_2^o & & & & & \\ & & & k_2^s & & & & \\ & & & & \ddots & & & \\ & & & & & \ddots & & \\ & & & & & & k_{N_s}^o & \\ & & & & & & & k_{N_s}^s \end{bmatrix}$$

$$K_m = \begin{bmatrix} k_1^o & 0 & k_{12}^{oo} & 0 & \cdots & k_{1N_s}^{oo} & 0 \\ 0 & k_1^s & 0 & 0 & & 0 & 0 \\ k_{21}^{oo} & 0 & k_2^o & 0 & & k_{1N_s}^{oo} & 0 \\ 0 & 0 & 0 & k_2^s & & 0 & 0 \\ \vdots & & & & \ddots & & \vdots \\ k_{N_s1}^{oo} & 0 & k_{N_s2}^{oo} & 0 & & k_{N_s}^o & 0 \\ 0 & 0 & 0 & 0 & \cdots & 0 & k_{N_s}^s \end{bmatrix}$$

Proof: The term $\boldsymbol{K}_d$ is a symmetric and positive definite matrix. Premultiplying both sides of Eq. (9) by $\boldsymbol{K}_d$ gives

$$(\boldsymbol{K}_d - \boldsymbol{K}_d\tilde{\Psi})\boldsymbol{D} = \boldsymbol{K}_d\tilde{\boldsymbol{T}}\eta \tag{10}$$

where

$$\boldsymbol{K}_d\tilde{\Psi} = \begin{bmatrix} 0 & -k_{12}^o & -k_{13}^o & \cdots & -k_{1N_s}^o \\ 0 & 0 & 0 & & 0 \\ -k_{21}^o & 0 & -k_{23}^o & & -k_{2N_{s_s}}^o \\ 0 & 0 & 0 & & 0 \\ \vdots & & & & \\ -k_{31}^o & -k_{32}^o & -k_3^o & & 0 \\ 0 & 0 & 0 & \cdots & 0 \end{bmatrix}$$

Furthermore, the submatrix $\boldsymbol{k}_{ij}^o$ can be partitioned into

$$\boldsymbol{k}_{ij}^o = \begin{bmatrix} \boldsymbol{k}_{ij}^{oo} & \boldsymbol{k}_{ij}^{os} \end{bmatrix}$$

where $\boldsymbol{k}_{ij}^{oo}$ and $\boldsymbol{k}_{ij}^{os}$ correspond to, respectively, the ordinary and actuator/sensor displacements of the jth subdomain. Because $\boldsymbol{d}_j^s \cap \boldsymbol{d}_j^b = \emptyset$, so that $\boldsymbol{k}_{ij}^{os} = 0$. Hence

$$\boldsymbol{K}_d(\boldsymbol{I} - \tilde{\Psi}) = \boldsymbol{K}_m \tag{11}$$

Rewriting $\boldsymbol{K}_m$ in the following form will not change its properties:

$$\tilde{\boldsymbol{K}}_m = \begin{bmatrix} \boldsymbol{k}_1^o & \boldsymbol{k}_{12}^{oo} & \cdots & \boldsymbol{k}_{1N_s}^{oo} & 0 & \cdots & 0 \\ \boldsymbol{k}_{21}^{oo} & \boldsymbol{k}_2^o & & \boldsymbol{k}_{1N_s}^{oo} & 0 & & 0 \\ \vdots & & \ddots & \vdots & \vdots & & \vdots \\ \boldsymbol{k}_{N_s1}^{oo} & \boldsymbol{k}_{N_s2}^{oo} & \cdots & \boldsymbol{k}_{N_s}^o & 0 & \cdots & 0 \\ 0 & 0 & \cdots & 0 & \boldsymbol{k}_1^s & \cdots & 0 \\ \vdots & & & \vdots & \vdots & \ddots & \vdots \\ 0 & 0 & \cdots & 0 & 0 & \cdots & \boldsymbol{k}_{N_s}^s \end{bmatrix}$$

It can be readily found that the upper partition of $\tilde{\boldsymbol{K}}_m$ is actually the reduced global stiffness matrix by simply crossing the columns and rows corresponding to the displacement vector $\boldsymbol{d}_j^s$ in the global stiffness matrix. Therefore it is a symmetric and positive definite matrix. The lower partition of $\tilde{\boldsymbol{K}}_m$ is nothing but the submatrix with all of the ordinary displacements constrained and is symmetric and positive definite, so that $\boldsymbol{K}_m$ is symmetric and positive definite. Therefore from Eq. (11) we have

$$\boldsymbol{I} - \tilde{\Psi} = \boldsymbol{K}_d^{-1}\boldsymbol{K}_m \Rightarrow (\boldsymbol{I} - \tilde{\Psi})^{-1} = \boldsymbol{K}_m^{-1}\boldsymbol{K}_d \tag{12}$$

The Theorem is therefore proved.

Calculation of $\boldsymbol{K}_m^{-1}\boldsymbol{K}_d$ could be expected to be much easier than that of $(\boldsymbol{I} - \tilde{\Psi})^{-1}$. Thus $\boldsymbol{D}$ can be solved from Eq. (9) as

$$\boldsymbol{D} = \boldsymbol{K}_m^{-1}\boldsymbol{K}_d\tilde{\boldsymbol{T}}\eta = \boldsymbol{T}\eta \tag{13}$$

Using Eq. (13), one can evaluate the reduced stiffness and mass matrices as

$$\boldsymbol{K}^* = \boldsymbol{T}^t\boldsymbol{K}\boldsymbol{T}, \qquad \boldsymbol{M}^* = \boldsymbol{T}^t\boldsymbol{M}\boldsymbol{T} \tag{14}$$

and the desired reduction of the eigenvalue problem of Eq. (1) can then be written as

$$\boldsymbol{K}^*\Phi^* - \boldsymbol{M}^*\Phi^*\Omega^* = 0 \tag{15}$$

where Φ^* is the eigenvector matrix, $\Omega^* = \mathrm{diag}\{\omega_1^{*2} \;\; \omega_2^{*2} \;\; \cdots \;\; \omega_{N_r}^{*2}\}$, and N_r is the reduced dimension.

It can be proved that if $N_r \to N$, then $\Omega^* \to \Omega$, and $\Phi^* \to \Phi$, where Ω and Φ are, respectively, the exact eigenvalue and eigenvector matrices of Eq. (1). This property guarantees the convergence of Eq. (15); i.e., if the dimension of the selected coordinate vector η is large enough, then accurate eigenpairs can be obtained.

Reduction of the Control Design System

Application of the transformation Eq. (13) to the control design problem Eq. (1) gives

$$\begin{aligned} \boldsymbol{M}^*\ddot{\eta} + \boldsymbol{C}^*\dot{\eta} + \boldsymbol{K}^*\eta &= \boldsymbol{T}^T\boldsymbol{B}_0\boldsymbol{u} \\ \boldsymbol{Y} &= \boldsymbol{S}_1\boldsymbol{T}\eta + \boldsymbol{S}_2\boldsymbol{T}\dot{\eta} \end{aligned} \tag{16}$$

Furthermore, making use of the transformation

$$\eta = \Phi^*\zeta \tag{17}$$

where ζ is a modal coordinate vector, Eq. (16) will become

$$\begin{aligned} \ddot{\zeta} + 2\xi\Omega^{*\frac{1}{2}}\dot{\zeta} + \Omega^*\zeta &= \Phi^{*T}\boldsymbol{T}^T\boldsymbol{B}_0\boldsymbol{u} \\ \boldsymbol{Y} &= \boldsymbol{S}_1\boldsymbol{T}\Phi^*\zeta + \boldsymbol{S}_2\boldsymbol{T}\Phi^*\dot{\zeta} \end{aligned} \tag{18}$$

where $\xi = \mathrm{diag}\{\xi_1 \;\; \xi_2 \;\; \cdots \;\; \xi_{N_r}\}$, the damping ratio matrix, and $\Omega^{*(1/2)} = \mathrm{diag}\{\omega_1^* \;\; \omega_2^* \;\; \cdots \;\; \omega_{N_r}^*\}$.

In summary, unlike the traditional CMS, there are no interface displacements in the final coordinate vector η in Eq. (13), meaning all DOF of a subdomain can be reduced. This is a significant advantage of the present method, especially where a large number of interface DOF have to be dealt with. Also, direct partitioning of Eq. (1) makes it easy to implement the subdomain method based on commercially available finite element method codes, because only the information about the global matrices is required. Finally, in attempting to maintain the integrity of the representation, the definition of these special displacements $\boldsymbol{d}_i^s$ may be extended to those of importance to the designer of the control system, an example of which could be the very localized DOF excited by impact loading or other minor physical nonlinearities.

Space Truss Structure

The space truss structure shown in Fig. 1 was analyzed. Properties of the members of the truss are as follows: Young's modulus $E = 10^7$ N/m^2, density $\rho = 2700$ kg/m^3, and cross-section area $A = 0.001$ m^2. Four added masses are attached at the third bay of the truss with value $m_a = 100$ kg, and four constant actuator forces with amplitude $p = 1000$ N act at the tip of the truss. The number of DOF of the complete model of the truss is 84. The truss structure is divided into two subdomains as shown in Fig. 2. The first subdomain has 36 DOF, but no actuator/sensor DOF, i.e., $n_{1s} = 0$. The second subdomain has 48 DOF and four actuator DOF, $n_{2s} = 4$. The reduced dimension for the truss is therefore $N_r = n_{1q} + n_{2q} + n_{2s}$.

Eigenvalues

The eigenvalue problem was solved for two different models: the complete model (CM) and the reduced model (RM) with $N_r = 34$. The present model shows a good agreement with the CM model for lower-order eigenpairs. A number of numerical experimental results have shown that the present model is likely to give higher eigenpairs,

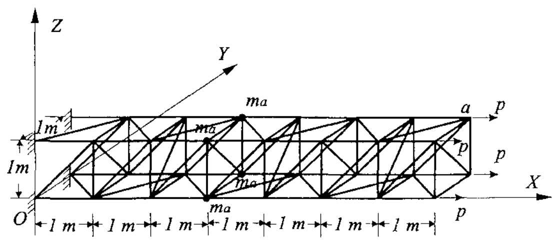

Fig. 1 Space truss structure with 91 members and 32 nodes.

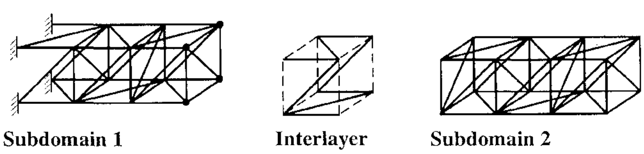

Fig. 2 Division of subdomains.

which are associated with localized actuator/sensor DOF. As shown in Fig. 3, the first 34 eigenvalues from the CM model are in the range 0–1000.0, whereas the 34 eigenvalues by the present model reach to 2000.0: 29 eigenvalues being located within the range from 0 to 1000.0 and 5 eigenvalues in the range from 1000.0 to 2000.0.

Dynamic Response

A direct assessment method for the RM is to check the open-loop response of the truss. This dynamic response was evaluated by three different methods: 1) direct superposition with all 84 modes of the CM model (DS84); 2) direct superposition with first $N_r = 34$ modes of the CM model (DS34); and 3) superposition with all 34 modes of the reduced model (SRM34). Using Duhamel's integral, an analytical solution can be obtained for individual modes with the given constant input. The solution of DS84 is nearly exact and is therefore used as a reference. For SRM34, values of $n_{1q} = 10$, $n_{2q} = 20$, and $n_{2s} = 4$ are considered.

When the locations of actuators/sensors are considered, the SRM34 is sensitive to the localized characteristics of the truss and can avoid losing information in the reduction procedure. This is demonstrated in Fig. 4, in which the horizontal displacement of node a, denoted as u_a, within the period 0 to $T_f = 0.01$ s is evaluated. The response of SRM34 is found to be much more accurate than that of DS34. To match the accuracy of SRM34 with direct superposition, at least 74 eigenmodes are required. This is because under impact loading higher-order modes associated with the actuators have been created; however, unlike SRM34, DS34 may not be able to take the effects of those higher-order modes into account. It is true that the accuracy of the solution by SRM34 may vary with the balance index of the DOF between the two subdomains. To investigate the influence of the balance index on the accuracy, we define $\varepsilon_r = \int_0^{T_f} |u_a^r - u_a^a|\,dt$ and $\varepsilon_s = \int_0^{T_f} |u_a^s - u_a^a|\,dt$ as the cumulative error in the response u_a during interval $[0, T_f]$, where u_a^r and u_a^s are the responses of u_a by SRM34 and DS34, respectively, and u_a^a by DS84. The balance index of the DOF is defined as $r = (n_{2q} + n_{2s})/N_r$; the larger the value of r, the more attention is paid to the second subdomain where all four actuators are located. To enhance our understanding, an increase in T_f from 0.01 to 0.1 s is investigated, and the cumulative error ε_r and ε_s against the index r is evaluated. It is shown in Fig. 5 that the cumulative error of u_a by SRM34 is less than that of DS34 for all of the values of r from 4/34 to 34/34. Higher values of r result in lower errors by SRM34, showing the importance of the impact localization.

The importance of the actuator/sensor related DOF is illustrated in Fig. 6, in which the extreme condition $n_{1q} = n_{2q} = 0$, i.e., $N_r = n_{2s} = 4$ is considered. It can be seen that the response u_a by direct superposition is incorrect, whereas the result by the present method compares well with the exact solution.

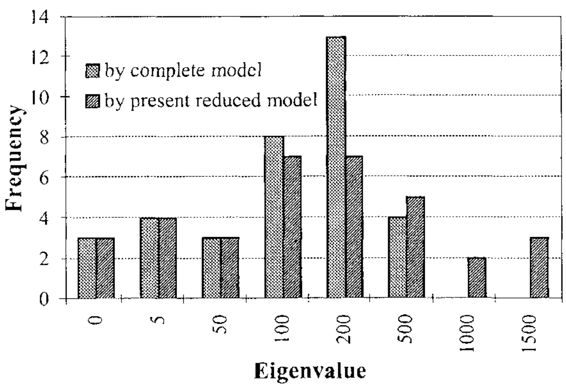

Fig. 3 Frequency diagram of the eigenvalues obtained by different models with N_r = 34.

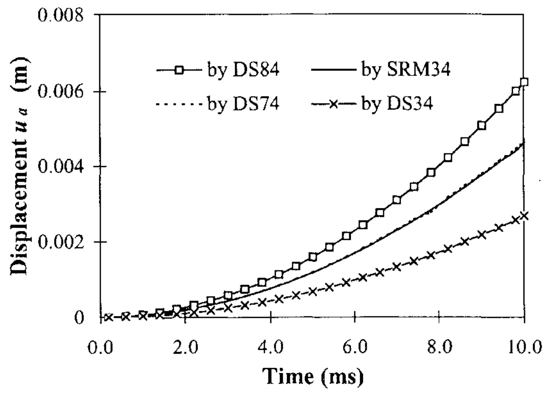

Fig. 4 Comparison of response u_a for 0.01 s impacting by four actuator forces.

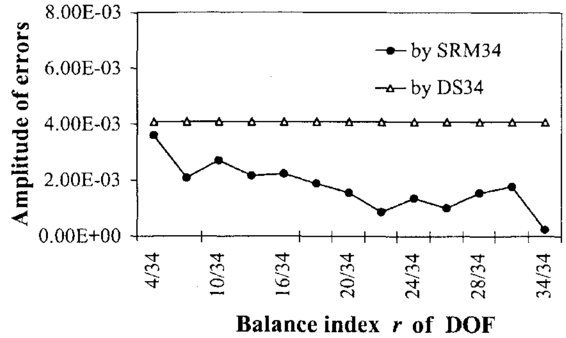

Fig. 5 Cumulative error of u_a by different methods for T_f = 0.1 s.

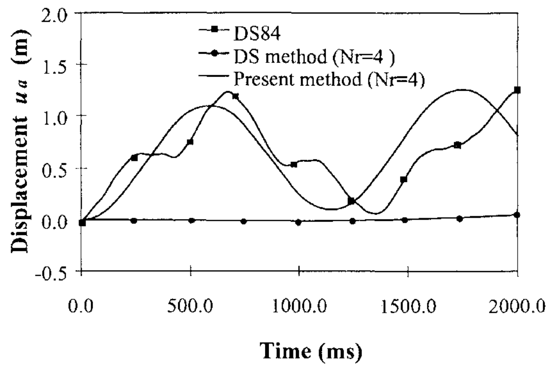

Fig. 6 Comparison of response u_a under extreme conditions of N_r = 4.

Conclusions

A generalized CB representation with consideration of actuators/sensors placement has been derived and used in the reduction of a control model applied to LSS. Detailed numerical simulation of an 84 DOF space truss has demonstrated the effectiveness of the representation. It has been found that the reduced model based on this representation can give satisfactory results for both mode synthesis and dynamic response analysis for the purpose of control system design. The importance of the actuator/sensor related DOF was studied under the extreme condition that only $N_r = 4$ DOF were considered. The numerical results have shown that the proposed approach can compensate for information ignored by traditional methods and provide acceptable results, whereas the direct superposition method totally failed in the computation.

Acknowledgment

The authors gratefully acknowledge the support of the Ministry of Education, Science, and Culture of Japan.

References

[1]Young, K. D., "Distributed Finite Element Modeling and Control Approach for Large Flexible Structures," *Journal of Guidance, Control, and Dynamics*, Vol. 13, No. 4, 1990, pp. 703–713.

[2]Park, K. C., and Belvin, W. K., "Partitioned Solution Procedure for Control-Structure Interaction Simulations," *Journal of Guidance, Control, and Dynamics*, Vol. 14, No. 1, 1991, pp. 59–67.

[3]Gregory, C. Z., Jr., "Reduction of Large Flexible Spacecraft Models Using Internal Balancing Theory," *Journal of Guidance, Control, and Dynamics*, Vol. 7, No. 5, 1984, pp. 725–732.

[4]Skelton, R. E., Hughes, P. C., and Hablani, H. B., "Order Reduction for Models of Space Structures Using Modal Cost Analysis," *Journal of Guidance, Control, and Dynamics*, Vol. 5, No. 5, 1982, pp. 351–357.

[5]Craig, R. R., Jr., and Bampton, M. C. C., "Coupling of Substructures for Dynamic Analysis," *AIAA Journal*, Vol. 6, No. 7, 1968, pp. 1313–1319.

[6]Triller, M. J., and Kammer, D. C., "Controllability and Observability Measures for Craig–Bampton Substructure Representations," *Journal of Guidance, Control, and Dynamics*, Vol. 17, No. 6, 1994, pp. 1198–1204.

[7]Su, T. J., and Craig, R. R., Jr., "Substructuring Decomposition and Controller Synthesis," AIAA Paper 90-1039, Aug. 1990.

[8]Onoda, J., Sano, T., and Kamiyama, K., "Active, Passive and Semiactive Vibration Suppression by Stiffness Variation," *AIAA Journal*, Vol. 30, No. 12, 1992, pp. 2922–2929.

[9]Onoda, J., and Haftka, R., "An Approach to Structure/Control Simultaneous Optimization for Large Flexible Spacecraft," *AIAA Journal*, Vol. 25, No. 8, 1987, pp. 1133–1138.